Fast-Twitch Glycolytic Skeletal Muscle Is Predisposed to Age-Induced Impairments in Mitochondrial Function

Robert A. Jacobs,[1,2,4] Víctor Díaz,[1–3] Lavinia Soldini,[4] Thomas Haider,[2] Martin Thomassen,[5] Nikolai B. Nordsborg,[5] Max Gassmann,[1,2,6] and Carsten Lundby[1,4]

[1]Zurich Center for Integrative Human Physiology (ZIHP) and
[2]Institute of Veterinary Physiology, Vetsuisse Faculty, University of Zurich, Switzerland.
[3]Department of Health and Human Performance, Universidad Politécnica de Madrid, Spain.
[4]Institute of Physiology, University of Zurich, Switzerland.
[5]Department of Exercise and Sport Sciences, University of Copenhagen, Copenhagen, Denmark.
[6]Universidad Peruana Cayetano Heredia (UPCH), Lima, Peru.

Address correspondence to Robert A. Jacobs, MSc, Institute of Veterinary Physiology and Zurich Center for Integrative Human Physiology (ZIHP), Winterthurerstrasse 260, CH-8057 Zurich, Switzerland. E-mail: jacobs@vetphys.uzh.ch

The etiology of mammalian senescence is suggested to involve the progressive impairment of mitochondrial function; however, direct observations of age-induced alterations in actual respiratory chain function are lacking. Accordingly, we assessed mitochondrial function via high-resolution respirometry and mitochondrial protein expression in soleus, quadricep, and lateral gastrocnemius skeletal muscles, which represent type 1 slow-twitch oxidative muscle (soleus) and type 2 fast-twitch glycolytic muscle (quadricep and gastrocnemius), respectively, in young (10–12 weeks) and mature (74–76 weeks) mice. Electron transport through mitochondrial complexes I and III increases with age in quadricep and gastrocnemius, which is not observed in soleus. Mitochondrial coupling efficiency during respiration through complex I also deteriorates with age in gastrocnemius and shows a tendency ($p = .085$) to worsen in quadricep. These data demonstrate actual alterations in electron transport function that occurs with age and are dependent on skeletal muscle type.

Key Words: Mitochondria—Respiratory chain—Function theory of aging.

Received October 2, 2012; Accepted December 19, 2012

Decision Editor: Rafael de Cabo, PhD

An inherent flaw of the bioenergetic reliance on aerobic metabolism to sustain life is the corollary oxidant production (1), and consequently mitochondria serve as the primary source of in vivo oxidant production (2–5). Mitochondria-derived reactive oxygen species are largely accounted for by superoxide (O_2^-) production into the mitochondrial matrix at mitochondrial complex I (CI) (6–8) and into both the matrix and mitochondrial intermembrane space at mitochondrial complex III (CIII) (9–14). The progression of reactive oxygen species production beyond hormetic concentrations precipitates deleterious and indiscriminate oxidation of nucleic acids, proteins, and lipids (5,15,16). These pernicious effects then correspondingly impair mitochondrial function, which result in greater oxidant production, and so on leading to a "vicious cycle" and eminent cellular demise (4,15,17). The mitochondrial theory of aging asserts that the biological aging process is facilitated by this progressive accrual of mitochondrial DNA (mtDNA) damage and reciprocal decline of mitochondrial function (18). Although evidence of increasing mtDNA alteration with age is supported by the literature, data suggestive of an impairment of mitochondrial function with aging are inconsistent.

Senescence corresponds with mounting indications of nuclear and mtDNA damage in both humans and animals (19–22). Moreover, mtDNA facilitated mutations lead to premature aging in mice (23) and humans (24). Transgenic studies show that reducing whole-body or tissue-specific mitochondrial superoxide dismutase, the enzyme that catalyses the dismutation of mitochondria-generated O_2^- to H_2O_2 (25), increases evidence of oxidative damage and premature aging (26–28). Alternatively, overexpression of endogenous mitochondrial catalase lessens oxidant damage, reduces an overall burden of disease (29), and increases life span (30). Indications of impaired mitochondrial function extending beyond measures of oxidant production or damage are lacking. Whether there are age-induced alterations in actual electron transport function remain unanswered (4).

Reports of functional impairments to mitochondria with aging are seemingly paradoxical. Mitochondrial enzymatic expression, protein synthesis, volume density, and oxidative capacity have been reported to decrease with age in humans and animals quadricep (QUAD) skeletal muscle (19,31–37) as well as in a collection of lower limb skeletal muscle representative of mixed glycolytic and oxidative fibers (38–40). The age-induced loss of mitochondrial protein expression and oxidative capacity, however, fails to decrease

in skeletal muscle primarily composed of type 2 fast-twitch glycolytic fibers (41–43). Modifications of mitochondrial content also differ with aging between *m. vastus lateralis* and *m. gastrocnemius* in humans (44). These differences have led to speculation that mitochondrial impairment with aging may differ across different skeletal muscle types (19,45). In vivo metabolic imaging techniques have provided preliminary evidence to support this assumption with skeletal muscle primarily composed of fast-twitch fibers exhibiting the greatest age-induced impairments (46,47).

Accordingly, the aim of this study is to examine mitochondrial protein expression along with analysis of respiratory capacity and control via high-resolution respirometry. Respirometric analyses using isolated mitochondrial preparations have been reported to exaggerate age-induced changes in mitochondrial function (48). Mitochondrial isolation techniques disturb native mitochondrial reticular networks in skeletal muscle (49) producing atypical and individual organelles through unregulated means (50–52). This alters innate mitochondrial characteristics (48,53–60) such as the loss of mitochondrial membrane integrity (61,62) and the ability to oxidize fatty acids (56). For respirometric analysis, we use saponin-permeabilized skeletal muscle preparations. This preparation allows for direct access to skeletal muscle mitochondria while maintaining both the cytocellular ultrastructure (51,63–68) and subcellular interactions with mitochondria (51,53,64,67–69). Cellular bioenergetics and metabolic channeling are predicated upon these factors (63,64,67,70). We have previously demonstrated that respirometric analysis using this in situ preparation in conjunction with biochemical assessment of mitochondria is more appropriate when attempting to differentiate between isolated changes in enzymatic expression versus an alteration in the functional capacity of a subcellular system (71–74). Accordingly, this specific mitochondrial preparation serves as the best model to examine respiratory capacity and control with aging. Respirometric analyses were carried out on soleus (SOL), QUAD, and lateral gastrocnemius (GAST) skeletal muscles, which represent type 1 slow-twitch oxidative muscle (SOL) and type 2 fast-twitch glycolytic muscle (QUAD and GAST), respectively, in young (10–12 weeks) and mature (74–76 weeks) mice. Taking into account the inconsistent reports of mitochondrial impairment with age across different skeletal muscles, we hypothesize that alterations in mitochondrial function with age vary across skeletal muscle types, explaining the seemingly inconsistent past findings on this topic.

Experimental Procedures

Ethical Approval

The experimental protocols using laboratory animals were approved by the Kantonales Veterinäramt Zürich (217/2010) and were performed in accordance with the Swiss animal protection laws and institutional guidelines.

Experimental Animals

A total of 24 male C57Bl/6 mice were used in the completion of this study, 12 young (10–12 week old) and 12 mature (74–76 week old) mice. All mice were housed in standard rodent cages (T3) with fixed temperature (21 ± 1°C), free access to food and water, and a 12-hour light–dark cycle. Animals were euthanized by means of carbon dioxide followed by rapid excision of SOL, QUAD, and GAST. These muscles represent a type 1 slow-twitch oxidative muscle (SOL) and a type 2 fast-twitch glycolytic muscle (QUAD and GAST), respectively. The skeletal muscles from one leg were quickly excised and placed in ice-cold biopsy solution for immediate respirometric analyses. The corresponding skeletal muscles from the opposite hind limb were then removed, frozen in liquid nitrogen, and stored at −80°C until processed for protein expression analysis (see Muscle Lysate Preparation, and Sodium Dodecyl Sulfate–Polyacrylamide Gel Electrophoresis and Western Blotting sections).

Muscle Lysate Preparation

The muscle samples were homogenized (Qiagen TissueLyser II, Retsch, Haan, Germany) in a fresh batch of buffer containing the following (in millimolar): 10% glycerol, 20 sodium-pyrophosphate, 150 NaCl, 50 4-(2-hydroxyethyl) piperazine-1-ethanesulfonic acid (HEPES) (pH 7.5), 1% NP-40, 20 β-glycerophosphate, 2 Na_3VO_4, 10 NaF, 2 phenylmethanesulfonyl fluoride, 1 ethylenediaminetetraacetic acid (pH 8.0), 1 ethylene glycol-bis(2-aminoethylether)-N,N,N′,N′-tetraacetic acid (EGTA) (pH 8.0), 10 µg/mL aprotinin, 10 µg/mL leupeptin, and 3 benzamidine. Afterward samples were rotated end over end for 1 hour at 4°C and centrifuged at 16,500*g* for 30 minutes at 4°C, and the supernatant (lysate) was used for further analysis. Total protein concentration in each sample was determined by a bovine serum albumin standard kit (Pierce, Rockford, IL), and all samples were diluted to the same protein concentration in ddH_2O and a modified 6× Laemmli buffer (7 mL 0.5 M Tris base [pH 6.8], 3 mL glycerol, 0.93 g dithiothreitol, 1 g sodium dodecyl sulfate, and 1.2 mg bromophenol blue).

Sodium Dodecyl Sulfate–Polyacrylamide Gel Electrophoresis and Western Blotting

Methods have been previously described in detail (75–77). Equal amounts (10 µg) of total muscle lysate proteins, determined during optimization of the different antibodies, were loaded in each well. Samples were loaded together with protein markers (Precision Plus All Blue and Dual Color, Bio-Rad Laboratories, Hercules, CA) on precasted gels (Bio-Rad Laboratories). Proteins were separated by sodium dodecyl sulfate–polyacrylamide gel electrophoresis and

semidry transferred to a polyvinylidene fluoride membrane (Millipore). The membranes were blocked in either 2% skimmed milk or 3% bovine serum albumin in Tris-buffered saline, including 0.1% Tween 20 before an overnight incubation in primary antibody at 4°C. Thereafter, membranes were washed in Tris-buffered saline, including 0.1% Tween 20 and incubated for 1 hour at room temperature in horseradish peroxidase-conjugated secondary antibody. Membranes were then washed 3 × 15 minutes in Tris-buffered saline, including 0.1% Tween 20 before the bands were visualized with ECL (Millipore) and recorded with a digital camera (ChemiDoc MP Imaging System, Bio-Rad). Quantification of the Western blot band intensity was done using the Image Lab software programme (Bio-Rad) and determined as the total band intensity minus the background intensity. Primary antibodies were optimized by use of mouse muscle lysates to secure that the protein amount loaded would result in band signal intensities localized on the steep and linearly part of a standard curve. To determine changes in total protein expression, the following antibodies were used with the localization of the quantified signal noted: 3-hydroxyacyl coenzyme a dehydrogenase (HAD): 83 kDa, polyclonal ab54477 (Abcam, UK); Mitochondrial Complex IV subunit 4, COXIV, (CIV): 16 kDa, monoclonal sc-58348 (Santa Cruz Biotechnology, Santa Cruz, CA); and Mitochondrial Complex I subunit NDUFB8 (CI): 20 kDa (monoclonal ab110242), Mitochondrial Complex II, Succinate Dehydrogenase complex subunit B (CII): 30 kDa (monoclonal ab14714), Mitochondrial Complex III subunit Core 2 (CIII): 45 kDa (monoclonal ab14745), Mitochondrial Complex V ATP Synthase subunit alpha (CV): 55 kDa (monoclonal ab14748) all four included in the MitoProfile Total OXPHOS Human WB Antibody Cocktail (ab110411, Abcam). The secondary antibodies used were horseradish peroxidase-conjugated goat anti-mouse and goat anti-rabbit (P-0447 and P-0448, DAKO, Denmark). All samples from the same muscle type were loaded on the same gel with young and mature muscles mixed. Signal intensity from each muscle sample was normalized to the mean signal intensity of the human standard.

Skeletal Muscle Preparation

Each part was immediately placed in ice-cold biopsy preservation solution containing 2.77 mM CaK_2EGTA buffer, 7.23 mM K_2EGTA buffer, 0.1 µM free calcium, 20 mM imidazole, 20 mM taurine, 50 mM 2-(*N*-morpholino) ethanesulfonic acid hydrate (K-MES), 0.5 mM dithiothreitol, 6.56 mM $MgCl_2$•$6H_2O$, 5.77 mM ATP, and 15 mM phosphocreatine (pH 7.1). Muscle samples were then gently dissected with a pair of fine-tipped forceps achieving a high degree of fiber separation verified microscopically. Chemical permeabilization followed via incubation in 2 mL of biopsy preservation solution with saponin (50 µg/mL) for 30 minutes in 4°C. Last, samples were washed with a mitochondrial respiration medium (MiR05) containing 0.5 mM EGTA, 3 mM $MgCl_2$•$6H_2O$, 60 mM K-lactobionate, 20 mM taurine, 10 mM KH_2PO_4, 20 mM HEPES, 110 mM sucrose, and 1 g/L bovine serum albumin (pH 7.1) for 10 minutes at 4°C.

Mitochondrial Respiration Measurements

Muscle bundles were blotted dry and measured for wet weight in a balance-controlled scale (XS205 DualRange Analytical Balance, Mettler-Toledo AG, Switzerland) maintaining constant relative humidity, providing hydration consistency as well as stability of weight measurements. Respiration measurements were performed in mitochondrial respiration medium 06 (MiR06; MiR05 + catalase 280 IU/mL). Measurements of oxygen consumption were performed at 37°C using the high-resolution Oxygraph-2k (Oroboros, Innsbruck, Austria) with all additions in each substrate, uncoupler, and inhibitor titration protocol added in series. Standardized instrumental calibrations were performed to correct for back diffusion of oxygen into the chamber from the various components, leak from the exterior, oxygen consumption by the chemical medium, and sensor oxygen consumption. Oxygen flux was resolved by software allowing nonlinear changes in the negative time derivative of the oxygen concentration signal (Oxygraph-2k, Oroboros). All experiments were carried out in a hyperoxygenated environment to prevent any potential oxygen diffusion limitation.

Respiratory Titration Protocols

Each titration protocol was specific to the examination of individual aspects of respiratory control through a sequence of coupling and substrate states induced via separate titrations, which were added in series as presented. The concentrations of substrates, uncouplers, and inhibitors used were based on prior experiments conducted for optimization of the titration protocols (71–73). A description of all three protocols is given in Table 1.

Table 1. Respirometric Titration Protocols

1	M: 2 mM	OC: 0.2 mM	ADP: 5 mM	G: 10 mM	S: 10 mM	Cyt C: 10 µM	FCCP: 1.5–3 µM	Rot: 0.5 µM	AmA: 2.5 µM
2	M: 2 mM	P: 5 mM	ADP: 5 mM	Cyt C: 10 µM	FCCP: 1.5–3 µM	Rot: 0.5 µM	AmA: 2.5 µM	—	—
3	Rot: 0.5 µM	S: 10 mM	ADP: 5 mM	Cyt C: 10 µM	FCCP: 1.5–3 µM	AmA: 2.5 µM	—	—	—

Notes: The three different titration protocols utilized in this study. Each row presents the substrate, uncoupler, or inhibitor and concentration titrated into the respiration medium, with all additions occurring sequentially as presented from left to right. ADP = adenosine diphosphate; AmA = antimycin A; Cyt C = cytochrome c; FCCP = carbonyl cyanide *p*-(trifluoromethoxy) phenylhydrazone; G = glutamate; M = malate; OC = octanoyl carnitine; Rot = rotenone; S = succinate.

Titration protocol 1

- Leak respiration in absence of adenylates (L_N) was induced with the addition of malate (2 mM) and octanoyl carnitine (0.2 mM). The L_N state represents the resting oxygen consumption of an unaltered and intact electron transport system (ETS) free of adenylates.
- Maximal electron flow through electron-transferring flavoprotein (ETF) and fatty acid oxidative capacity, P_{ETF}, were both determined following the addition of ADP (5 mM). In the P_{ETF} state, the ETF-linked transfer of electrons requires the metabolism of acetyl-CoA, hence the addition of malate, in order to facilitate convergent electron flow into the Q-junction from both CI and ETF allowing β-oxidation to proceed. The contribution of electron flow through CI is far below capacity and so here the rate-limiting metabolic branch is electron transport through ETF such that malate + octanoyl carnitine + ADP-stimulated respiration is representative of, rather than specific to, electron capacity through ETF (71,78,79).
- Submaximal state 3 respiratory capacity specific to CI, P_{CI}, was induced following the additions of glutamate (10 mM).
- Maximal state 3 respiration, oxidative phosphorylation capacity, P, was then induced with the addition of succinate (10 mM). P demonstrates a naturally intact ETS's capacity to catalyze a sequential set of redox reactions that are partially coupled to the production of ATP via ATP Synthase. P maintains an electrochemical gradient across the inner mitochondrial membrane dictated by the degree of coupling to the phosphorylation system (63,65). This maximal state 3 state represents respiration that is resultant to saturating concentrations of ADP and substrate supply for both CI and succinate dehydrogenase, CII. Convergent electron input to CI and CII provides higher respiratory values compared with the isolated respiration of either CI (pyruvate and/or glutamate + malate or glutamate + malate) or CII (succinate + rotenone) (63, 80). Consequently, P presents more physiological relevance to the study of mitochondrial function (81) and is necessary to establish confirmation of a complete and intact ETS.
- As an internal control for compromised integrity of the mitochondrial preparation, the mitochondrial outer membrane was assessed with the addition of cytochrome c (10 µM). If respiration significantly increased following titration of cytochrome c, then the measurement was removed and not included in statistical analysis. There was no indication of mitochondrial damage in the measurements included in the study as demonstrated by the average 3.5%, 2.9%, 7.5%, 5.3%, 6.3%, and 2.3% change in young and mature QUAD, SOL, and GAST respiration, respectively. All were either below or within the accepted 5%–15% elevation in respiration following exogenous cytochrome c titration, successfully verifying the integrity of the outer mitochondrial membrane (64).
- Phosphorylative restraint of electron transport was assessed by uncoupling ATP Synthase, CV from the ETS with the titration of the proton ionophore, and carbonyl cyanide *p*-(trifluoromethoxy) phenylhydrazone (0.5 µM per addition up to optimum concentrations ranging from 1.5 to 3 µM) reaching ETS capacity. The inner mitochondrial membrane potential is completely collapsed with an open transmembrane proton circuit in the ETS respiratory state. The uninhibited flow of electrons through the respiratory system can, therefore, indirectly serve as an indication of maximal mitochondrial membrane potential.
- Finally, rotenone (0.5 µM) and antimycin A (2.5 µM) were added, in sequence, to terminate respiration by inhibiting CI and CIII, respectively. With CI inhibited, electron flow is specific to CII, providing submaximal state 3 respiration through CII (P_{CII}).
- Inhibition of respiration with antimycin A then allows for the determination and correction of residual oxygen consumption, indicative of nonmitochondrial oxygen consumption in the chamber.

Titration protocol 2.—This titration protocol was necessary for determination of coupling control of electrons through CI.

- L_N–malate (2 mM) and pyruvate (5 mM).
- P_{CI}–ADP (5 mM).
- Internal control for mitochondrial outer membrane integrity–cytochrome c (10 µM). There was no indication of mitochondrial damage in the measurements included in the study as demonstrated by the 0.3%, 1.3%, 0.1%, –0.3%, 4.3%, and –0.1% change in mouse young and mature QUAD, SOL, and GAST respiration, respectively.
- ETS–carbonyl cyanide *p*-(trifluoromethoxy) phenylhydrazone (0.5 µM per addition up to optimum concentrations ranging from 1.5 to 3 µM).
- CI inhibition–rotenone (0.5 µM).
- Residual oxygen consumption–antimycin A (2.5 µM).

Titration protocol 3.—This titration protocol was necessary for determination of coupling control of electrons through CII.

- CI inhibition–rotenone (0.5 µM).
- L_N–succinate (10 mM).
- P_{CII}–ADP (5 mM).
- Internal control for mitochondrial outer membrane integrity–cytochrome c (10 µM). There was no indication of mitochondrial damage in the measurements included in the study as demonstrated by the 7.3%, 2.6%, 9.8%, 13.4%, 5.1%, and 7.3% change in mouse young and mature QUAD, SOL, and GAST respiration, respectively.

- ETS–carbonyl cyanide *p*-(trifluoromethoxy) phenylhydrazone (0.5 μM per addition up to optimum concentrations ranging from 1.5 to 3 μM).
- Residual oxygen consumption–antimycin A (2.5 μM).

Respirometric values representing P_{CI} and P_{CII} did not differ across titration protocols. Consequently all P_{CI} and P_{CII} values achieved with the titration protocols for 2 and 3, respectively, were grouped with complementing respiratory state from titration protocol 1.

Data Analysis

All mass-specific respirometric values were controlled to account for the differences in mitochondrial content, as indicated by CII protein expression, across age and fiber types. In doing so, all CII protein expression data were adjusted to a value of 1. The degree by which the protein expression had to be adjusted to equal 1 was then applied to all mass-specific respirometric values corresponding with the appropriate age and skeletal muscle type, respectively. Values of P_{CI} controlling for CI protein expression, P_{ETF} controlling for HAD protein expression, and P controlling for CIII protein expression all were also adjusted using the same method.

For all statistical evaluations, a p value of less than .05 was considered significant. Differences in respiratory capacities and protein expression with age and across skeletal muscle groups were initially compared using a two-way analysis of variance. When an analysis of variance was significant, differences in respiratory capacities and protein expression with age and across skeletal muscle groups were evaluated using pairwise comparisons with a Bonferroni adjustment (SPSS Statistics 17.0, SPSS, Inc., Chicago, IL). Indices of mitochondrial efficiency did not express a Gaussian distribution and therefore a Kruskal–Wallis analysis of variance and the U-Mann Whitney tests were used to reveal differences between younger and older muscle as well as comparisons across muscle groups within the respective age groups.

Results

Skeletal Muscle Protein Expression

As shown in Figure 1, protein expression for all mitochondrial enzymes was greatest in the slow-twitch SOL muscle. In young animals only the expression of CII and CIV differed between QUAD and GAST, both of which were lost with age. Only SOL expressed a change in mitochondrial protein content with age as CI, CII, and CV all increased (Figure 1A, B, and E, respectively). Though no significant changes in protein expression of CIII (Figure 1C) or CIV (Figure 1D) were apparent, both complexes showed a tendency to diminish with age in GAST (p = .060 and .063, respectively). Collectively, this analysis illustrates that the protein content for enzymes involved in mitochondrial oxidative phosphorylation is largely unaffected in primarily fast-twitch glycolytic muscle (QUAD and GAST) but slightly increased in primarily slow-twitch oxidative muscle (SOL) with age.

Mitochondrial Respiration

Main effects of age on mass-specific respiration (pmol O_2/min/mg ww) were observed for P_{ETF} (p = .011) and P_{CII} (p = .008). This was reflected by the higher P_{ETF} and P_{CII} in mature QUAD (p = .031 and .037, respectively; Figure 2E) and GAST (p = .011 and .016, respectively; Figure 2I) versus their younger counterparts. There was also a main effect of muscle type on mass-specific respiration as SOL has greater respiration across all states compared with both QUAD and GAST (p < .001; Figure 2A).

Mass-specific respiration does not take into account differences in mitochondrial content between samples (Figure 1). Accordingly, all respirometric analyses were adjusted for CII protein content, a biomarker shown to express the best concordance with mitochondrial content and total cristae area as measured by transmission electron microscopy as well as myocellular respiratory capacity over protein concentrations for all other mitochondrial complexes (82). When controlling respiration to mitochondrial content, the main effect of age on respiration capacity (pmol O_2/min/CII) appeared to be silenced by the divergent fluctuations in mitochondrial function across skeletal muscle types in response to age. Respiratory states representing P_{CI}, P, and ETS in QUAD and P_{CI}, P, ETS, and P_{CII} in SOL all lost respiratory capacity in response to age (Figure 2F and H). Conversely, GAST increased respiratory capacity at every respiratory state measured (Figure 2J) in response to age. The differences in respiratory capacity when controlling for mitochondrial content across skeletal muscle in younger and older mice are shown in Figure 2B and D, respectively.

Respiratory Capacity and Coupling Control Specific to Mitochondrial Complexes I and III

Electron transport and control specifically through CI and CIII are of particular interest as reactive oxygen species production at each respective complex accounts for the majority of mitochondria-specific oxidant production (9–14). In order to isolate analysis to these specific complexes, all P_{CI} values, including respirometric values from both titration protocols 1 and 2, and maximal state 3 respirometric values, P, were adjusted to account for the differences in CI and CIII protein expression, respectively, with age and across muscle groups (Figure 1A and C).

There were main effects of age (p = .001) on P_{C1} respiration when controlling for CI expression (pmol O_2/min/CI), which increased with age in both QUAD and GAST (p < .001) and decreased in SOL (p = .003; Figure 3A–C). The

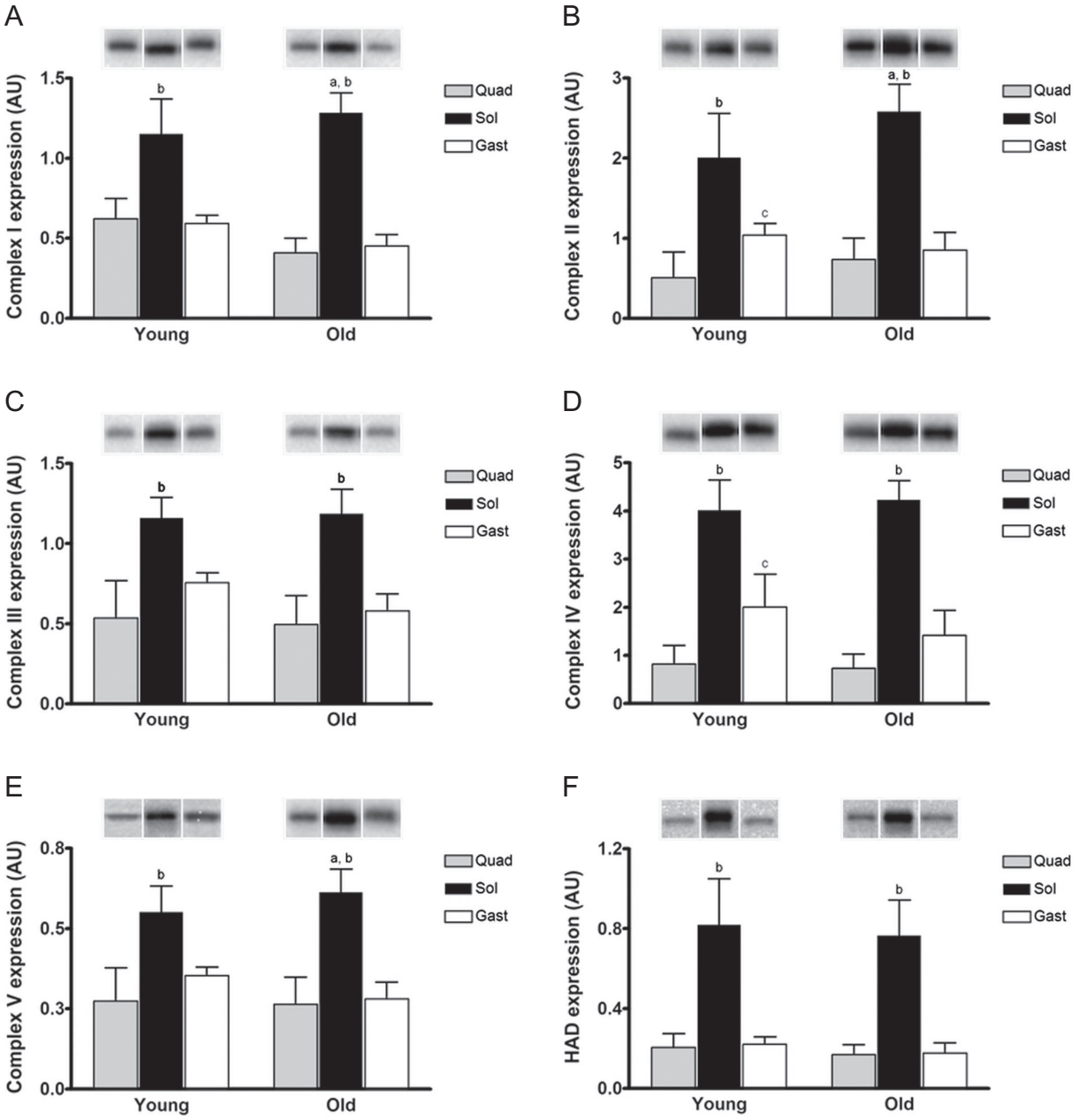

Figure 1. Protein expression of mitochondrial complexes and proteins with age. Skeletal muscle protein expression determined in young (10–12 weeks) and mature (74–76 weeks) C57Bl/6 mice. Protein expression for (A) CI, mitochondrial complex I or NADH dehydrogenase; (B) CII, mitochondrial complex II or succinate dehydrogenase; (C) CIII, mitochondrial complex III or cytochrome bc_1 complex; (D) CIV, mitochondrial complex IV or cytochrome c oxidase; (E) CV, mitochondrial complex V or ATP Synthase; and (F) HAD, 3-hydroxyacyl coenzyme a dehydrogenase, is illustrated in response to age and across skeletal muscles. Example blots for one analysis from one animal are shown above the graph. Values are means ± *SD*. In figure, a indicates significant difference in age within a skeletal muscle, $p < .05$; b shows significant difference between soleus (black) from both quadricep (grey) and lateral gastrocnemius (white) within the same age, $p < .05$; and c indicates differences between quadricep and gastrocnemius within the same age, $p < .05$.

coupling efficiency during P_{CI} respiration deteriorated with age in GAST ($p = .043$) and showed a tendency to diminish in QUAD as well ($p = .085$; Table 2). Though no differences in respiratory capacity were observed across all young muscle groups during P_{CI} when controlling for CI, the coupling control was superior in young QUAD and GAST over SOL ($p = .021$ and .009, respectively). In the older muscle both QUAD and GAST presented with higher P_{CI} than SOL ($p < .001$) and both, again, expressed a tighter coupling efficiency than SOL ($p = .004$ and $p < .001$).

There were also main effects of age ($p = .009$) on maximal state 3 respiration and oxidative phosphorylation capacity, P, when controlling for CIII protein expression (pmol O_2/min/CIII) (Figure 4A–C). Respiration capacity in both QUAD and GAST increased with age ($p = .009$ and .001, respectively), whereas SOL did not change ($p = .144$).

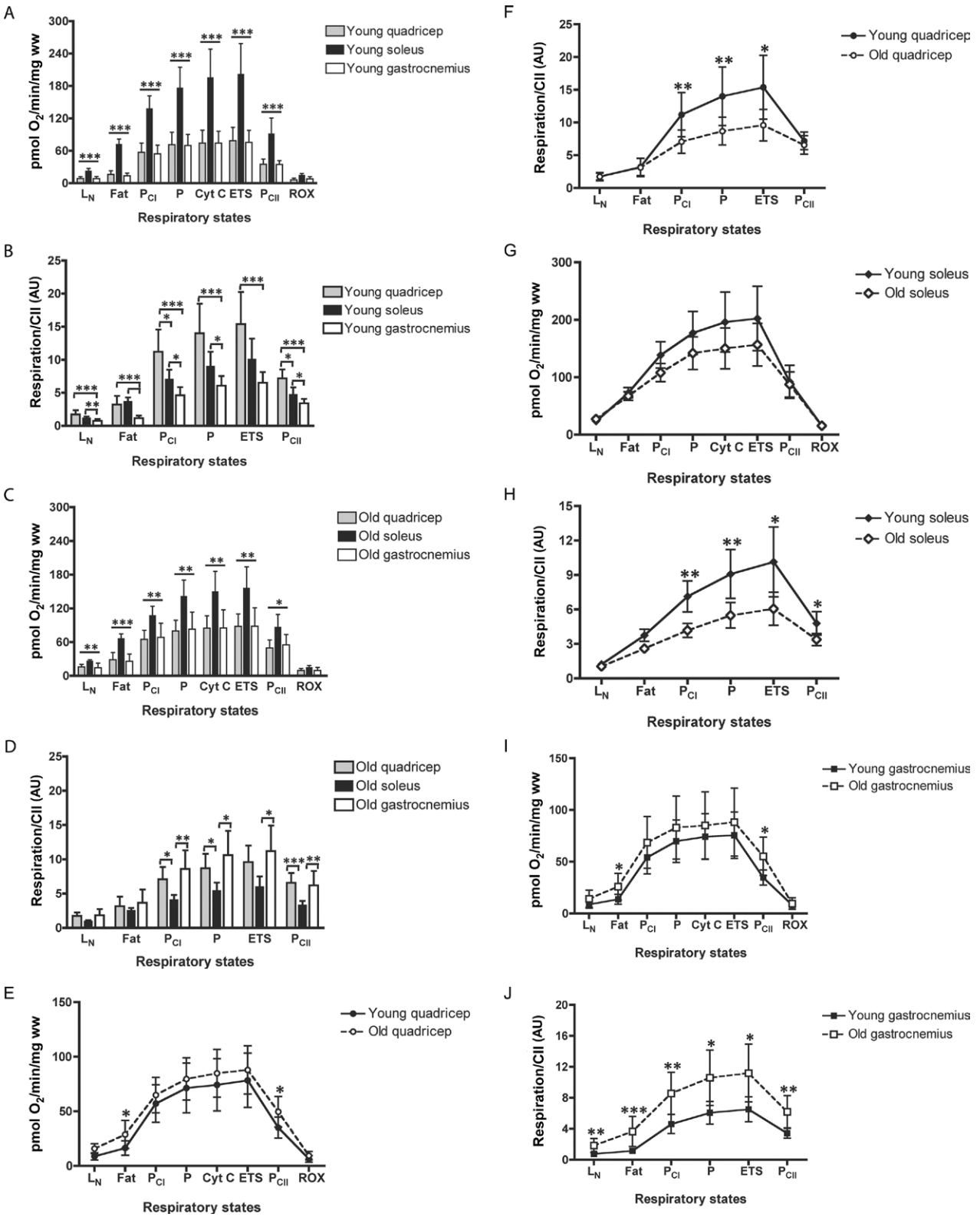

Figure 2. Skeletal muscle respirometric analysis. Mass-specific respiration across muscle groups in (A) young and (C) mature animals. Mass-specific respiration with age in mouse (E) quadricep, (G) soleus, and (I) gastrocnemius skeletal muscles. Mitochondrial-specific respiration controlling for mitochondrial content, as assessed by mitochondrial complex II protein expression (82), across skeletal muscles in (B) young and (D) mature animals. Mitochondrial-specific respiration with age in mouse (F) quadricep, (H) soleus, and (J) gastrocnemius skeletal muscles. L_N, leak respiration without adenylates; P_{EFT}, maximal fatty acid oxidation; P_{CI}, submaximal state 3 respiration through mitochondrial complex I (CI); P, maximal state 3 respiration–oxidative phosphorylation capacity; Cyt C, cytochrome c, internal test of mitochondrial membrane integrity; ETS, electron transport system capacity; and P_{CII}, submaximal state 3 respiration through mitochondrial complex II (CII). Data presented as mean ± *SD*. *, **, and *** indicate significant difference of $p \leq .05$, $p \leq .01$, and $p \leq .001$, respectively.

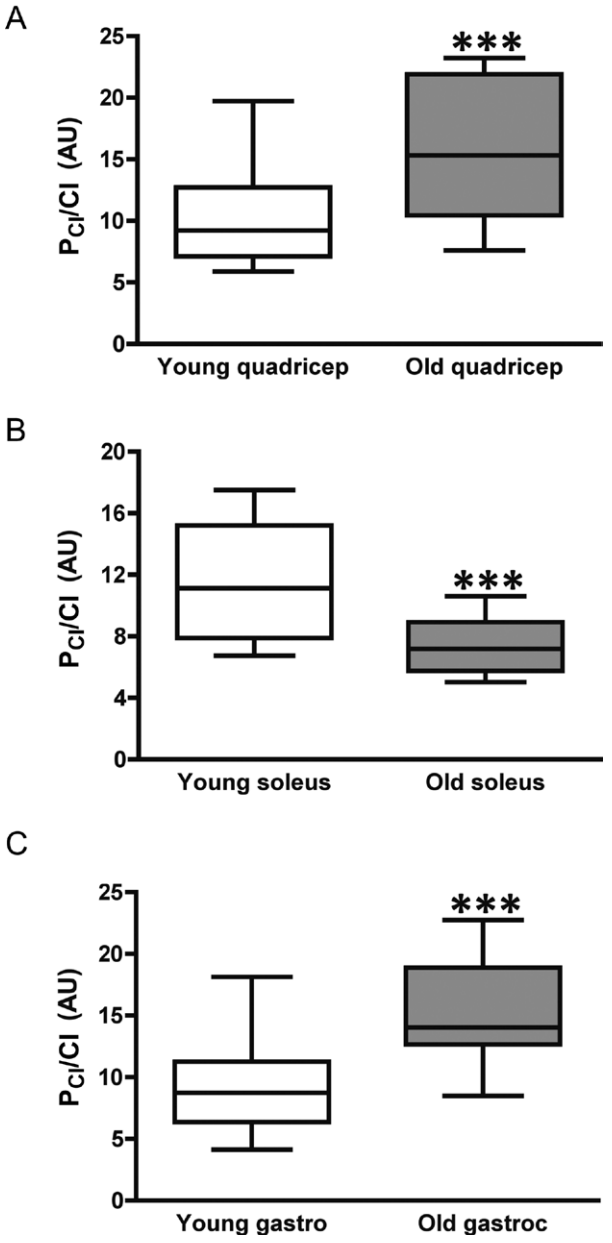

Figure 3. Respiratory capacity and control through mitochondrial complex I (CI). Submaximal state 3 respiratory capacity specific to CI (P_{CI}) when controlling for CI protein expression with age in (A) quadricep, (B) soleus, and (C) gastrocnemius skeletal muscles. *, **, and *** indicate significant difference of age, $p \leq .05$, $p \leq .01$, and $p \leq .001$, respectively.

Differences across young muscle groups were evident between both QUAD and SOL versus GAST ($p = .023$ and .001, respectively) and across mature muscle groups with QUAD greater than SOL ($p = .020$).

Respiratory Capacity and Control Specific to β-Oxidation

Only values of fatty acid oxidative capacity, P_{ETF}, were adjusted to account for the differences in HAD protein expression (Figure 1D). P_{ETF} (pmol O_2/min/HAD) increased with age in QUAD ($p = .004$) and showed a tendency to increase in GAST ($p = .065$) (Figure 5). Differences across young and mature muscle groups were evident with both QUAD and GAST far below SOL ($p < .001$). Though P_{ETF}, when controlling for HAD, did not change in SOL (Figure 5), the coupling efficiency during β-oxidation diminished with age (Table 2). Despite this decrease with age, the coupling control of electron transport during β-oxidation in SOL was significantly better than younger and older QUAD ($p = .01$ and .05, respectively). Coupling control during fat oxidation did not change with age in QUAD or GAST, though it did differ between young SOL and GAST ($p = .05$). This difference was lost with age (Table 2).

Discussion

The aim of this study was to analyze the effect of biological aging on respiratory capacities and mitochondrial coupling control across different skeletal muscle types as a function of age. Our main findings are (i) mitochondrial function is dependent on skeletal muscle type, irrespective of age; (ii) submaximal state 3 respiration specific to CI, P_{CI}, increased in both QUAD and GAST but decreased in SOL when controlling for complex I protein expression; (iii) coupling control during P_{CI} was also lost with age in GAST and indicated a tendency for deterioration in QUAD but remained unchanged in SOL; (iv) maximal state 3 respiration and oxidative phosphorylation capacity, P, increased with age in QUAD and GAST but not SOL when controlling for CIII protein expression; and finally (v) although the capacity for fat respiration increased with age in QUAD when controlling for differences in HAD protein expression across skeletal muscle types, the

Table 2. Mitochondrial Coupling Efficiency With Age

	Young QUAD	Mature QUAD	Young SOL	Mature SOL	Young GAST	Mature GAST
LCR_{ETF}	0.54 ± 0.16†	0.53 ± 0.18†	0.33 ± 0.09*,†,‡	0.41 ± 0.05*,†	0.57 ± 0.29‡	0.52 ± 0.10
LCR_{CI}	0.15 ± 0.03†,§	0.20 ± 0.07†,§	0.24 ± 0.11†,‡	0.29 ± 0.06†,‡	0.12 ± 0.06*,‡	0.17 ± 0.03*,‡
LCR_{CII}	0.69 ± 0.13	0.76 ± 0.07	0.54 ± 0.25	0.72 ± 0.11	0.68 ± 0.19	0.66 ± 0.11

Notes: Leak control ratios (LCR) as indices of mitochondrial coupling and respiratory control across different skeletal muscles with age. GAST = gastrocnemius; LCR_{ETF} = coupling efficiency of electron transfer through electron-transferring flavoprotein (ETF) during β-oxidation; P_{CI} = coupling efficiency of electron transfer during respiration through mitochondrial complex I (CI); P_{CII} = coupling efficiency of electron transfer during respiration through mitochondrial complex II (CII); QUAD = quadriceps; SOL = soleus.

*,†,‡Effect of age, difference between QUAD vs SOL, and difference in SOL vs GAST, respectively, with $p < .05$.

§Difference with age, $p = .085$. Data are presented as mean ± *SD*.

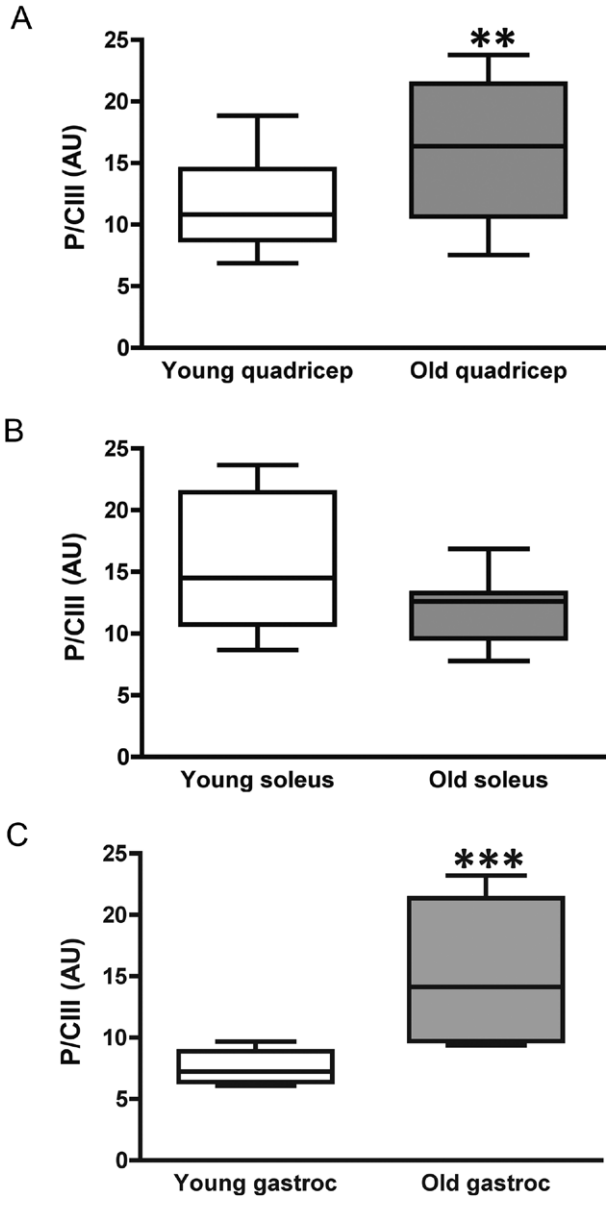

Figure 4. Respiratory capacity and control through mitochondrial complex III (CIII). Maximal state 3 respiration and oxidative phosphorylation capacity (P) when controlling for CIII protein expression with age in (A) quadricep, (B) soleus, and (C) gastrocnemius skeletal muscles. *, **, and *** indicate significant difference of age, $p \leq .05$, $p \leq .01$, and $p \leq .001$, respectively.

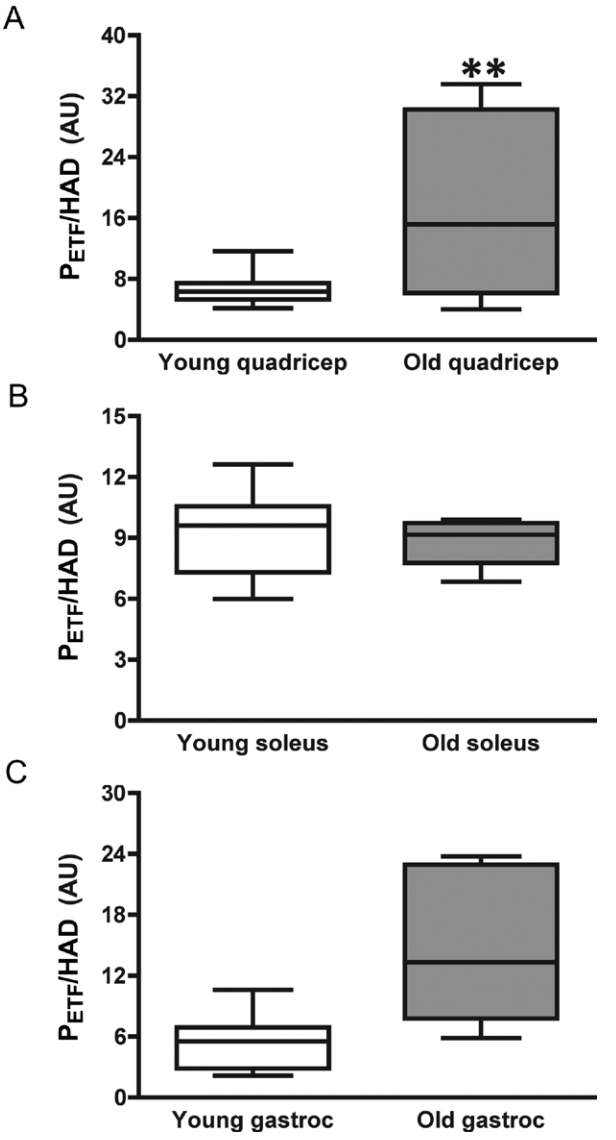

Figure 5. Respiratory capacity and control through electron transferring flavoprotein (ETF) during maximal fat respiration. Submaximal state 3 respiratory capacity specific to the capacity for fat oxidation and electron transfer through ETF (P_{ETF}) when controlling for 3-hydroxyacyl coenzyme a dehydrogenase (HAD) protein expression with age in (A) quadricep, (B) soleus, and (C) gastrocnemius skeletal muscles. *, **, and *** indicate significant difference of age, $p \leq .05$, $p \leq .01$, and $p \leq .001$, respectively. # indicates a tendency of a difference with age, $p = .065$.

coupling control during fat oxidation worsened with age only in SOL.

Variations in Mitochondrial Function Across Fiber Types

There is some dispute on whether differences in respiratory capacity fluctuate across different skeletal muscle types that vary in their biochemical makeup, tailoring oxidative function to specific metabolic demand (83). Initial reports suggested that respiratory differences could be accounted for simply by the differences in mitochondrial content (50,84). This has since been refuted as various skeletal muscles have been shown to express respiratory differences across muscle types (46,47,85,86). We recently substantiated these differences in mitochondrial function across muscle types as respiration capacities in both GAST and QUAD were greater than those in SOL at P_{CI}, P_{CII}, P, and ETS respiratory states when normalizing mass-specific respiration to citrate synthase activity (87). Although it seems evident that differences in function exist across different skeletal muscle fiber types, even when controlling for the disproportionate expression of mitochondria, the data

presented here demonstrate how important normalization of the mass-specific respirometric values can be to overall data interpretation.

Our findings specific to mitochondrial protein expression are contrary to studies suggestive of a progressive loss of mitochondria with age (34,48). We cannot exclude the possibility that some mitochondrial protein/fragments may have been lost as a result of our homogenization and centrifugation procedures. Thus, we cannot confirm that our mitochondrial protein determination is representative of the total per volume of muscle mass, possibly explaining the differences between studies. Alternatively, however, our results are in accordance with several studies reporting negligible to minor changes in mitochondrial protein expression with age, including an increase of expression that is dependent on skeletal muscle type (32,33,45,88). There is also evidence in mice of *increased* skeletal muscle mitochondrial protein synthesis with advancing age (88). Although it is unlikely that the preferential loss of mitochondrial protein during homogenization and centrifugation procedures biased our results, we cannot definitively exclude this possibility.

Skeletal Muscle Mitochondrial Respiratory Capacity and Control Across Skeletal Muscle Types With Age

Mitochondrial respiratory capacities across several different states diminished with age in QUAD and SOL (Figure 2F and H). These results coincide with previous reports where oxidative capacity is reported to decline with age in either QUAD or mixed muscle homogenates (19,31,33,35,36,38,39). Alternatively, mitochondrial respiratory capacities across all states increased with age in GAST (Figure 2J). The increase in respiratory capacity with age in GAST also corresponds with previous work that demonstrated a greater reliance with age of oxidative phosphorylation for ATP synthesis in primarily type 2 fast-twitch glycolytic skeletal muscle (41,42,89).

Mitochondria serve as a primary source of in vivo oxidant production (2–5) with the primary oxidant production occurring at CI (6–8) and CIII (9–14). Despite the macro decreases in mitochondrial-specific respiratory capacity in QUAD (Figure 2F), respiration and electron flow specifically through CI and CIII increased (Figures 3A and 4A). Coupling control during P_{CI} also had a tendency to deteriorate in QUAD ($p = .085$) in response to age (Table 2). Respiration and electron flow specifically through CI and CIII also increased in GAST, whereas coupling control during P_{CI} worsened with age (Table 2). Electron coupling control is indicative of oxidant production as mitochondrial production of superoxide is closely related to mitochondrial coupling efficiency during respiration (9). Moreover, increased mitochondrial respiration capacity also results in increased oxidative damage and shorter life span (27). Respiratory capacity through CI diminished, whereas capacity through CIII and electron coupling control through CI remained unaffected by age in the slow-twitch oxidative SOL (Figures 3B and 4B, and Table 2, respectively). Highly glycolytic skeletal muscle has been shown to have higher oxidant production with a reciprocal lower capacity for oxidant scavenging compared with highly oxidative muscle (90). Predominantly fast-twitch skeletal muscle also has been reported to accrue age-associated oxidative damage, as assessed with protein carbonyl profiles across different skeletal muscle types, more rapidly than slow-twitch oxidative muscle (91). Collectively, the results from this study, in corroboration with these previous findings, provide the direct evidence of a predisposition to ETS dysfunction with age in type 2 fast-twitch glycolytic skeletal muscle that is not observed in type 1 slow-twitch oxidative muscle and has been previously suggested in humans using indirect metabolic imaging techniques (46,47). Preliminary evidence suggests that caloric restriction (92) and exercise (93) reduce mitochondrial oxidant production and may serve to counterbalance these age-related impairments in electron transport.

Ratios of coupling control are based on the supposition that a tightly coupled system can be distinguished from a dyscoupled system by the magnitude of difference between two steady respiratory states with identical substrate supply (94). We used leak control ratios as our indices of mitochondrial coupling control efficiency (Table 2). Leak control ratios are produced between two reciprocal respiratory states; a low flux state (ie, L_N with malate and pyruvate, state 4 respiration) compared with an equivalent high respiratory flux state (ie, P_{CI}, submaximal state 3 respiration). An identical substrate supply is necessary to pair corresponding states. Flux control ratios demonstrate coupling efficiency using a theoretical minimum of 0.0, which indicates a fully coupled system, to a value of 1.0 representing a fully noncoupled or dyscoupled system (63). Although we show evidence of a loss of coupling control with aging during P_{CI} in GAST and a tendency in QUAD, unfortunately coupling efficiency during maximal state 3 respiration could not be determined with the titration protocols utilized as there was no reciprocal leak state measured for P.

Respiratory Capacity and Control of Fat Oxidation With Aging

We found that the capacity for fat respiration increased with age without a reciprocal loss of coupling efficiency during β-oxidation in QUAD when controlling for differences in HAD protein expression (Figure 5 and Table 2, respectively). Conversely, capacity for fat respiration was unaltered with age in SOL, though the coupling control during fat oxidation diminished. Neither respiratory capacity nor control of fat oxidation was altered in GAST. Skeletal muscle intramyocellular lipid stores increase in

parallel with age-related decreases in mitochondria (37). Moreover, intramyocellular lipid content is also reported to drift away from the mitochondrial reticulum with age (37). The dysregulation of fat metabolism within skeletal muscle is associated with the development of insulin resistance and metabolic disease (95–97). The loss of mitochondrial coupling efficiency in type 1 slow-twitch fibers, such as observed here, may in part explain the reported insulin resistance in healthy, lean, elderly participants (38). This is of interest in regards to metabolic disease as well as aging and merits further investigation.

Conclusions

Here, we directly demonstrate impairments of mitochondrial function in response to aging in skeletal muscle. The specific age-induced alteration in function is dependent on skeletal muscle type. Skeletal muscle composed primarily of type 2 fast-twitch glycolytic fibers are predisposed to progressive impairments in mitochondrial function with age as type 1 slow-twitch oxidative fibers appear to protect against this effect.

Author Contributions

All respirometric measurements were performed at the Institute of Physiology at University of Zurich (R.A.J., V.D., L.S.), whereas the Western blot analyses were done at the Department of Exercise and Sport Sciences at University of Copenhagen (M.T.). The following is a list stating the contribution of each author to specific aspects of the study: (i) Conception and design of the experiments (R.A.J. and C.L.); (ii) Contribution of reagents, facilities, and analytical tools (T.H., N.B.N., M.G., and C.L.); (iii) Collection of data (R.A.J., V.D., L.S., and M.T.); (iv) Analysis and interpretation of data (R.A.J., V.D., M.T.); and (v) Drafting the article or revising it critically for important intellectual content (R.A.J., V.D., T.H., M.T., N.B.N., M.G., and C.L.).

References

1. Harman D. Aging: a theory based on free radical and radiation chemistry. *J Gerontol*. 1956;11:298–300.
2. Beckman KB, Ames BN. The free radical theory of aging matures. *Physiol Rev*. 1998;78:547–581.
3. Wallace DC. Mitochondrial diseases in man and mouse. *Science*. 1999;283:1482–1488.
4. Balaban RS, Nemoto S, Finkel T. Mitochondria, oxidants, and aging. *Cell*. 2005;120:483–495.
5. Turrens JF. Mitochondrial formation of reactive oxygen species. *J Physiol (Lond)*. 2003;552:335–344.
6. Kussmaul L, Hirst J. The mechanism of superoxide production by NADH:ubiquinone oxidoreductase (complex I) from bovine heart mitochondria. *Proc Natl Acad Sci USA*. 2006;103:7607–7612.
7. Kushnareva Y, Murphy AN, Andreyev A. Complex I-mediated reactive oxygen species generation: modulation by cytochrome c and NAD(P)+ oxidation-reduction state. *Biochem J*. 2002;368:545–553.
8. Turrens JF, Boveris A. Generation of superoxide anion by the NADH dehydrogenase of bovine heart mitochondria. *Biochem J*. 1980;191:421–427.
9. Yin Y, Yang S, Yu L, Yu CA. Reaction mechanism of superoxide generation during ubiquinol oxidation by the cytochrome bc1 complex. *J Biol Chem*. 2010;285:17038–17045.
10. Chen Q, Vazquez EJ, Moghaddas S, Hoppel CL, Lesnefsky EJ. Production of reactive oxygen species by mitochondria: central role of complex III. *J Biol Chem*. 2003;278:36027–36031.
11. Turrens JF, Alexandre A, Lehninger AL. Ubisemiquinone is the electron donor for superoxide formation by complex III of heart mitochondria. *Arch Biochem Biophys*. 1985;237:408–414.
12. Guzy RD, Hoyos B, Robin E, et al. Mitochondrial complex III is required for hypoxia-induced ROS production and cellular oxygen sensing. *Cell Metab*. 2005;1:401–408.
13. Han D, Williams E, Cadenas E. Mitochondrial respiratory chain-dependent generation of superoxide anion and its release into the intermembrane space. *Biochem J*. 2001;353:411–416.
14. Muller FL, Liu Y, Van Remmen H. Complex III releases superoxide to both sides of the inner mitochondrial membrane. *J Biol Chem*. 2004;279:49064–49073.
15. Jacobs HT. The mitochondrial theory of aging: dead or alive? *Aging Cell*. 2003;2:11–17.
16. Stadtman ER, Levine RL. Protein oxidation. *Ann N Y Acad Sci*. 2000;899:191–208.
17. Bishop NA, Lu T, Yankner BA. Neural mechanisms of ageing and cognitive decline. *Nature*. 2010;464:529–535.
18. Fleming JE, Miquel J, Cottrell SF, Yengoyan LS, Economos AC. Is cell aging caused by respiration-dependent injury to the mitochondrial genome? *Gerontology*. 1982;28:44–53.
19. Short KR, Bigelow ML, Kahl J, et al. Decline in skeletal muscle mitochondrial function with aging in humans. *Proc Natl Acad Sci USA*. 2005;102:5618–5623.
20. Hamilton ML, Van Remmen H, Drake JA, et al. Does oxidative damage to DNA increase with age? *Proc Natl Acad Sci USA*. 2001;98:10469–10474.
21. Michikawa Y, Mazzucchelli F, Bresolin N, Scarlato G, Attardi G. Aging-dependent large accumulation of point mutations in the human mtDNA control region for replication. *Science*. 1999;286:774–779.
22. Shigenaga MK, Hagen TM, Ames BN. Oxidative damage and mitochondrial decay in aging. *Proc Natl Acad Sci USA*. 1994;91:10771–10778.
23. Trifunovic A, Wredenberg A, Falkenberg M, et al. Premature ageing in mice expressing defective mitochondrial DNA polymerase. *Nature*. 2004;429:417–423.
24. Payne BA, Wilson IJ, Hateley CA, et al. Mitochondrial aging is accelerated by anti-retroviral therapy through the clonal expansion of mtDNA mutations. *Nat Genet*. 2011;43:806–810.
25. McCord JM, Fridovich I. Superoxide dismutase. An enzymic function for erythrocuprein (hemocuprein). *J Biol Chem*. 1969;244:6049–6055.
26. Melov S, Schneider JA, Day BJ, et al. A novel neurological phenotype in mice lacking mitochondrial manganese superoxide dismutase. *Nat Genet*. 1998;18:159–163.
27. Kokoszka JE, Coskun P, Esposito LA, Wallace DC. Increased mitochondrial oxidative stress in the Sod2 (+/-) mouse results in the age-related decline of mitochondrial function culminating in increased apoptosis. *Proc Natl Acad Sci USA*. 2001;98:2278–2283.
28. Esposito LA, Melov S, Panov A, Cottrell BA, Wallace DC. Mitochondrial disease in mouse results in increased oxidative stress. *Proc Natl Acad Sci USA*. 1999;96:4820–4825.
29. Treuting PM, Linford NJ, Knoblaugh SE, et al. Reduction of age-associated pathology in old mice by overexpression of catalase in mitochondria. *J Gerontol A Biol Sci Med Sci*. 2008;63:813–822.
30. Schriner SE, Linford NJ, Martin GM, et al. Extension of murine life span by overexpression of catalase targeted to mitochondria. *Science*. 2005;308:1909–1911.
31. Conley KE, Jubrias SA, Esselman PC. Oxidative capacity and ageing in human muscle. *J Physiol (Lond)*. 2000;526(Pt 1):203–210.
32. Larsen S, Hey-Mogensen M, Rabøl R, Stride N, Helge JW, Dela F. The influence of age and aerobic fitness: effects on mitochondrial respiration in skeletal muscle. *Acta Physiol (Oxf)*. 2012;205:423–432.
33. Rasmussen UF, Krustrup P, Kjaer M, Rasmussen HN. Experimental evidence against the mitochondrial theory of aging. A study of

isolated human skeletal muscle mitochondria. *Exp Gerontol*. 2003;38:877–886.
34. Rooyackers OE, Adey DB, Ades PA, Nair KS. Effect of age on in vivo rates of mitochondrial protein synthesis in human skeletal muscle. *Proc Natl Acad Sci USA*. 1996;93:15364–15369.
35. Tonkonogi M, Fernström M, Walsh B, et al. Reduced oxidative power but unchanged antioxidative capacity in skeletal muscle from aged humans. *Pflugers Arch*. 2003;446:261–269.
36. Trounce I, Byrne E, Marzuki S. Decline in skeletal muscle mitochondrial respiratory chain function: possible factor in ageing. *Lancet*. 1989;1:637–639.
37. Crane JD, Devries MC, Safdar A, Hamadeh MJ, Tarnopolsky MA. The effect of aging on human skeletal muscle mitochondrial and intramyocellular lipid ultrastructure. *J Gerontol A Biol Sci Med Sci*. 2010;65:119–128.
38. Petersen KF, Befroy D, Dufour S, et al. Mitochondrial dysfunction in the elderly: possible role in insulin resistance. *Science*. 2003;300:1140–1142.
39. Hepple RT, Hagen JL, Krause DJ, Jackson CC. Aerobic power declines with aging in rat skeletal muscles perfused at matched convective O2 delivery. *J Appl Physiol*. 2003;94:744–751.
40. Figueiredo PA, Ferreira RM, Appell HJ, Duarte JA. Age-induced morphological, biochemical, and functional alterations in isolated mitochondria from murine skeletal muscle. *J Gerontol A Biol Sci Med Sci*. 2008;63:350–359.
41. Lanza IR, Befroy DE, Kent-Braun JA. Age-related changes in ATP-producing pathways in human skeletal muscle in vivo. *J Appl Physiol*. 2005;99:1736–1744.
42. Lanza IR, Larsen RG, Kent-Braun JA. Effects of old age on human skeletal muscle energetics during fatiguing contractions with and without blood flow. *J Physiol (Lond)*. 2007;583:1093–1105.
43. Chretien D, Gallego J, Barrientos A, et al. Biochemical parameters for the diagnosis of mitochondrial respiratory chain deficiency in humans, and their lack of age-related changes. *Biochem J*. 1998;329(Pt 2):249–254.
44. Houmard JA, Weidner ML, Gavigan KE, Tyndall GL, Hickey MS, Alshami A. Fiber type and citrate synthase activity in the human gastrocnemius and vastus lateralis with aging. *J Appl Physiol*. 1998;85:1337–1341.
45. Picard M, Ritchie D, Thomas MM, Wright KJ, Hepple RT. Alterations in intrinsic mitochondrial function with aging are fiber type-specific and do not explain differential atrophy between muscles. *Aging Cell*. 2011;10:1047–1055.
46. Conley KE, Amara CE, Jubrias SA, Marcinek DJ. Mitochondrial function, fibre types and ageing: new insights from human muscle in vivo. *Exp Physiol*. 2007;92:333–339.
47. Amara CE, Shankland EG, Jubrias SA, Marcinek DJ, Kushmerick MJ, Conley KE. Mild mitochondrial uncoupling impacts cellular aging in human muscles in vivo. *Proc Natl Acad Sci USA*. 2007;104:1057–1062.
48. Picard M, Ritchie D, Wright KJ, et al. Mitochondrial functional impairment with aging is exaggerated in isolated mitochondria compared to permeabilized myofibers. *Aging Cell*. 2010;9:1032–1046.
49. Kirkwood SP, Munn EA, Brooks GA. Mitochondrial reticulum in limb skeletal muscle. *Am J Physiol*. 1986;251:C395–C402.
50. Schwerzmann K, Hoppeler H, Kayar SR, Weibel ER. Oxidative capacity of muscle and mitochondria: correlation of physiological, biochemical, and morphometric characteristics. *Proc Natl Acad Sci USA*. 1989;86:1583–1587.
51. Picard M, Taivassalo T, Gouspillou G, Hepple RT. Mitochondria: isolation, structure and function. *J Physiol (Lond)*. 2011;589:4413–4421.
52. Benz R. Porin from bacterial and mitochondrial outer membranes. *CRC Crit Rev Biochem*. 1985;19:145–190.
53. Milner DJ, Mavroidis M, Weisleder N, Capetanaki Y. Desmin cytoskeleton linked to muscle mitochondrial distribution and respiratory function. *J Cell Biol*. 2000;150:1283–1298.
54. Kunz WS, Kudin A, Vielhaber S, Elger CE, Attardi G, Villani G. Flux control of cytochrome c oxidase in human skeletal muscle. *J Biol Chem*. 2000;275:27741–27745.
55. Villani G, Greco M, Papa S, Attardi G. Low reserve of cytochrome c oxidase capacity in vivo in the respiratory chain of a variety of human cell types. *J Biol Chem*. 1998;273:31829–31836.
56. Pande SV, Blanchaer MC. Preferential loss of ATP-dependent long-chain fatty acid activating enzyme in mitochondria prepared using Nagarse. *Biochim Biophys Acta*. 1970;202:43–48.
57. Brooks GA. Lactate shuttle – between but not within cells? *J Physiol (Lond)*. 2002;541:333–334.
58. Brooks GA, Hashimoto T. Investigation of the lactate shuttle in skeletal muscle mitochondria. *J Physiol (Lond)*. 2007;584:705–706; author reply 707–708.
59. Chretien D, Pourrier M, Bourgeron T, et al. An improved spectrophotometric assay of pyruvate dehydrogenase in lactate dehydrogenase contaminated mitochondrial preparations from human skeletal muscle. *Clin Chim Acta*. 1995;240:129–136.
60. Horan MP, Pichaud N, Ballard JW. Review: quantifying mitochondrial dysfunction in complex diseases of aging. *J Gerontol A Biol Sci Med Sci*. 2012;67:1022–1035.
61. Benz R. Permeation of hydrophilic solutes through mitochondrial outer membranes: review on mitochondrial porins. *Biochim Biophys Acta*. 1994;1197:167–196.
62. Wicker U, Bücheler K, Gellerich FN, Wagner M, Kapischke M, Brdiczka D. Effect of macromolecules on the structure of the mitochondrial inter-membrane space and the regulation of hexokinase. *Biochim Biophys Acta*. 1993;1142:228–239.
63. Gnaiger E. Capacity of oxidative phosphorylation in human skeletal muscle: new perspectives of mitochondrial physiology. *Int J Biochem Cell Biol*. 2009;41:1837–1845.
64. Kuznetsov AV, Veksler V, Gellerich FN, Saks V, Margreiter R, Kunz WS. Analysis of mitochondrial function in situ in permeabilized muscle fibers, tissues and cells. *Nat Protoc*. 2008;3:965–976.
65. Pesta D, Gnaiger E. High-resolution respirometry. OXPHOS protocols for human cells and permeabilized fibers from small biopsies of human muscle. *Mitochondria Bioenergy Meth Protocols*. 2011;810:25–58.
66. Saks VA, Belikova YO, Kuznetsov AV. In vivo regulation of mitochondrial respiration in cardiomyocytes: specific restrictions for intracellular diffusion of ADP. *Biochim Biophys Acta*. 1991;1074:302–311.
67. Saks VA, Veksler VI, Kuznetsov AV, et al. Permeabilized cell and skinned fiber techniques in studies of mitochondrial function in vivo. *Mol Cell Biochem*. 1998;184:81–100.
68. Lin A, Krockmalnic G, Penman S. Imaging cytoskeleton–mitochondrial membrane attachments by embedment-free electron microscopy of saponin-extracted cells. *Proc Natl Acad Sci USA*. 1990;87:8565–8569.
69. Veksler VI, Kuznetsov AV, Sharov VG, Kapelko VI, Saks VA. Mitochondrial respiratory parameters in cardiac tissue: a novel method of assessment by using saponin-skinned fibers. *Biochim Biophys Acta*. 1987;892:191–196.
70. Kay L, Nicolay K, Wieringa B, Saks V, Wallimann T. Direct evidence for the control of mitochondrial respiration by mitochondrial creatine kinase in oxidative muscle cells in situ. *J Biol Chem*. 2000;275:6937–6944.
71. Jacobs RA, Boushel R, Wright-Paradis C, et al. Mitochondrial function in human skeletal muscle following high altitude exposure. *Exp Physiol*. 2012. doi:10.1113/expphysiol.2012.066092
72. Jacobs RA, Lundby C. Mitochondria express enhanced quality as well as quantity in association with aerobic fitness across recreationally active individuals up to elite athletes. *J Appl Physiol*. 2012. doi:10.1152/japplphysiol.01081.2012
73. Jacobs RA, Rasmussen P, Siebenmann C, et al. Determinants of time trial performance and maximal incremental exercise in highly trained endurance athletes. *J Appl Physiol*. 2011;111:1422–1430.

74. Jacobs RA, Siebenmann C, Hug M, Toigo M, Meinild AK, Lundby C. 28 days at 3,454 m altitude diminishes respiratory capacity but enhances efficiency in human skeletal muscle mitochondria. *FASEB J*. 2012. doi:10.1096/fj.12-218206.
75. Nordsborg NB, Siebenmann C, Jacobs RA, et al. Four weeks of normobaric "live high-train low" do not alter muscular or systemic capacity for maintaining pH and K^+ homeostasis during intense exercise. *J Appl Physiol*. 2012;112:2027–2036.
76. Nordsborg N, Ovesen J, Thomassen M, et al. Effect of dexamethasone on skeletal muscle Na+,K+ pump subunit specific expression and K+ homeostasis during exercise in humans. *J Physiol (Lond)*. 2008;586:1447–1459.
77. Thomassen M, Rose AJ, Jensen TE, et al. Protein kinase Cα activity is important for contraction-induced FXYD1 phosphorylation in skeletal muscle. *Am J Physiol Regul Integr Comp Physiol*. 2011;301:R1808–R1814.
78. Eaton S, Bartlett K, Pourfarzam M. Mammalian mitochondrial beta-oxidation. *Biochem J*. 1996;320(Pt 2):345–357.
79. Lanza IR, Nair KS. Mitochondrial function as a determinant of life span. *Pflugers Arch*. 2010;459:277–289.
80. Rasmussen UF, Rasmussen HN. Human quadriceps muscle mitochondria: a functional characterization. *Mol Cell Biochem*. 2000;208:37–44.
81. Brand MD, Nicholls DG. Assessing mitochondrial dysfunction in cells. *Biochem J*. 2011;435:297–312.
82. Larsen S, Nielsen J, Hansen CN, et al. Biomarkers of mitochondrial content in skeletal muscle of healthy young human subjects. *J Physiol (Lond)*. 2012;590:3349–3360.
83. Picard M, Hepple RT, Burelle Y. Mitochondrial functional specialization in glycolytic and oxidative muscle fibers: tailoring the organelle for optimal function. *Am J Physiol Cell Physiol*. 2012;302:C629–C641.
84. Hoppeler H, Hudlicka O, Uhlmann E. Relationship between mitochondria and oxygen consumption in isolated cat muscles. *J Physiol (Lond)*. 1987;385:661–675.
85. Jackman MR, Willis WT. Characteristics of mitochondria isolated from type I and type IIb skeletal muscle. *Am J Physiol*. 1996;270:C673–C678.
86. Picard M, Csukly K, Robillard ME, et al. Resistance to Ca2+-induced opening of the permeability transition pore differs in mitochondria from glycolytic and oxidative muscles. *Am J Physiol Regul Integr Comp Physiol*. 2008;295:R659–R668.
87. Jacobs RA, Diaz V, Meinild AK, Gassmann M, Lundby C. The C57Bl/6 mouse serves as a suitable model of human skeletal muscle mitochondrial function. *Exp Physiol*. 2012. doi:10.1113/expphysiol.2012.07003.
88. Miller BF, Robinson MM, Bruss MD, Hellerstein M, Hamilton KL. A comprehensive assessment of mitochondrial protein synthesis and cellular proliferation with age and caloric restriction. *Aging Cell*. 2012;11:150–161.
89. Lanza IR, Russ DW, Kent-Braun JA. Age-related enhancement of fatigue resistance is evident in men during both isometric and dynamic tasks. *J Appl Physiol*. 2004;97:967–975.
90. Anderson EJ, Neufer PD. Type II skeletal myofibers possess unique properties that potentiate mitochondrial H(2)O(2) generation. *Am J Physiol Cell Physiol*. 2006;290:C844–C851.
91. Feng J, Navratil M, Thompson LV, Arriaga EA. Principal component analysis reveals age-related and muscle-type-related differences in protein carbonyl profiles of muscle mitochondria. *J Gerontol A Biol Sci Med Sci*. 2008;63:1277–1288.
92. Chen Y, Hagopian K, McDonald RB, et al. The influence of dietary lipid composition on skeletal muscle mitochondria from mice following 1 month of calorie restriction. *J Gerontol A Biol Sci Med Sci*. 2012;67:1121–1131.
93. Alves RM, Vitorino R, Figueiredo P, Duarte JA, Ferreira R, Amado F. Lifelong physical activity modulation of the skeletal muscle mitochondrial proteome in mice. *J Gerontol A Biol Sci Med Sci*. 2010;65:832–842.
94. Chance B, Williams GR. Respiratory enzymes in oxidative phosphorylation. III. The steady state. *J Biol Chem*. 1955;217:409–427.
95. Amati F, Dubé JJ, Alvarez-Carnero E, et al. Skeletal muscle triglycerides, diacylglycerols, and ceramides in insulin resistance: another paradox in endurance-trained athletes? *Diabetes*. 2011;60:2588–2597.
96. Chomentowski P, Coen PM, Radiková Z, Goodpaster BH, Toledo FG. Skeletal muscle mitochondria in insulin resistance: differences in intermyofibrillar versus subsarcolemmal subpopulations and relationship to metabolic flexibility. *J Clin Endocrinol Metab*. 2011;96:494–503.
97. Coen PM, Goodpaster BH. Role of intramyocelluar lipids in human health. *Trends Endocrinol Metab*. 2012;23:391–398.